

Assessment of water quality and quantity of springs at a pilot-scale: Applications in semi-arid Mediterranean areas in Lebanon

Joanna Doummar¹, Marwan Fahs², Michel Aoun¹, Reda Elghawi¹, Jihad Othman¹, Mohamad Alali¹, and Assaad H. Kassem¹

¹American University of Beirut

²Strasbourg University

November 22, 2022

Abstract

This work presents an integrated methodology for the assessment of threats on spring quality and quantity in poorly investigated Mediterranean semi-arid karst catchments in Lebanon. Pilot investigations, including 1) high-resolution monitoring of spring water and climate, 2) artificial tracer experiments, and 3) analysis of micropollutants in surface water, groundwater, and wastewater samples were conducted to assess flow and transport in three karst catchments of El Qachqouch, El Assal, and Laban springs. First, the high-resolution in-situ spring data allows the quantification of available water volumes, as well as their seasonal and yearly variability in addition to shortages and floodwaters. Moreover, the statistical analysis of hydrographs and chemographs helps assess the karst typology, spring type and hydrodynamic behavior (storage versus fast flow). Furthermore, a series of artificial tracer experiments provides information about key-transport parameters related to the intrinsic vulnerability of the pilot springs, while the analysis of micropollutants gives insight into the specific types of point source pollution as well as contaminant types and loads. On the one hand, the tracer experiments reveal that any potential contamination occurring in snow-governed areas can be observed at the spring for an extensive time due to its intermittent release by gradual snowmelt, even with enough dilution effect. On the other hand, the assessment of persistent wastewater indicators shows that springs in the lower catchment (including El Qachqouch) are highly vulnerable to a wide range of pollutants from point source (dolines and river) and diffuse percolation. Such contaminants breakthrough is challenging to predict because of the heterogenous duality of infiltration and flow, typical of karst systems. Finally, this set of investigations is essential for the proper characterization of poorly studied systems in developing areas, whereby results can be integrated into conceptual and numerical models to be used by decision-makers as support tools in science-evidenced management plans.

1 **Assessment of water quality and quantity of springs at a pilot-scale: Applications in semi-**
2 **arid Mediterranean areas in Lebanon**

3 **Joanna Doummar*¹, Marwan Fahs², Michel Aoun¹, Reda Elghawi¹, Jihad Othman¹,**
4 **Mohamad Alali¹, and Assaad H. Kassem¹.**

5 ¹ Department of Geology, American University of Beirut, Beirut, Lebanon; *Corresponding
6 author jd31@aub.edu.lb

7 ²Institut Terre et Environnement de Strasbourg, Université de Strasbourg, CNRS, ENGEES,
8 UMR 7063, 67084 Strasbourg, France

9 **Keywords**

10 Karst methods, springs, tracer experiment, monitoring, micropollutants, Mediterranean

11 **Abstract**

12 This work presents an integrated methodology for the assessment of threats on spring quality and
13 quantity in poorly investigated Mediterranean semi-arid karst catchments in Lebanon. Pilot
14 investigations, including 1) high-resolution monitoring of spring water and climate, 2) artificial
15 tracer experiments, and 3) analysis of micropollutants in surface water, groundwater, and
16 wastewater samples were conducted to assess flow and transport in three karst catchments of El
17 Qachqouch, El Assal, and Laban springs. First, the high-resolution in-situ spring data allows the
18 quantification of available water volumes, as well as their seasonal and yearly variability in
19 addition to shortages and floodwaters. Moreover, the statistical analysis of hydrographs and
20 chemographs helps assess the karst typology, spring type and hydrodynamic behavior (storage
21 versus fast flow). Furthermore, a series of artificial tracer experiments provides information
22 about key-transport parameters related to the intrinsic vulnerability of the pilot springs, while the
23 analysis of micropollutants gives insight into the specific types of point source pollution as well

24 as contaminant types and loads. On the one hand, the tracer experiments reveal that any
25 potential contamination occurring in snow-governed areas can be observed at the spring for an
26 extensive time due to its intermittent release by gradual snowmelt, even with enough dilution
27 effect. On the other hand, the assessment of persistent wastewater indicators shows that springs
28 in the lower catchment (including El Qachqouch) are highly vulnerable to a wide range of
29 pollutants from point source (dolines and river) and diffuse percolation. Such contaminants
30 breakthrough is challenging to predict because of the heterogenous duality of infiltration and
31 flow, typical of karst systems. Finally, this set of investigations is essential for the proper
32 characterization of poorly studied systems in developing areas, whereby results can be integrated
33 into conceptual and numerical models to be used by decision-makers as support tools in science-
34 evidenced management plans.

35 **1. Introduction**

36 Freshwater, notably groundwater is presently under tremendous stresses due to climate change
37 and variability in addition to the increase of urbanization, contamination, water needs, and
38 demands (Hou et al., 2013, Jongman, 2014, Kløve et al., 2014, Van Loon et al., 2017, Luo et al.,
39 2020). The Mediterranean region has been identified as one of the most vulnerable areas in terms
40 of increase in forecasted air temperatures and precipitation (Diffenbaugh and Giorgi, 2012,
41 Goderniaux et al., 2015, Nerantzaki and Nikolaidis, 2020), expected to affect drastically water
42 resources in semi-arid regions (Iglesias et al., 2007, Doummar et al., 2018b, Dubois et al., 2020,
43 Marin et al., 2021, Sivelle et al., 2021). Karst aquifers predominant in the Mediterranean (Chen
44 et al., 2017) provide about 25% of the water supply worldwide (Ford and Williams, 2007,
45 Stevanovic, 2019a). Mediterranean karst catchment areas characterized by limited surface runoff
46 and high infiltration rates reaching 70% are drained by one or multiple springs (Doummar et al.,

47 2012a, 2018, Hartmann et al., 2014,2015). Due to the duality of flow and heterogeneities in karst
48 systems, flow and transport occur in highly permeable conduits draining a low permeability
49 matrix (Geyer et al., 2008, Mudarra et al., 2010). Generally, the breakthrough of contaminants in
50 karst springs varies according to the dynamic conditions in the aquifer (Doummar et al., 2018a)
51 and the type of pollutant (Hillebrand et al., 2012, Doummar et al., 2014, Doummar and Aoun
52 2018b). While transport may occur rapidly because of fast flow velocities (Pronk et al. 2006,
53 Bailly-Comte et al. 2010), the flow rates increasing exponentially during a short period as a
54 response to high rain events will induce a high dilution, thus reducing the concentration of
55 contaminants in the spring (Chang et al., 2020). Given this complexity, the spring responsive
56 behavior, often highly variable to climatic conditions and hydraulic properties of the aquifer, is
57 very difficult to predict in the long and short-run (Sivelle et al., 2021). Chen et al., 2018 show
58 that the total flow rates of a karst spring in an Alpine setting will substantially decrease under the
59 different climatic scenarios mostly because of the shift in snowmelt patterns. Nerantzaki and
60 Nikolaidis, (2020) found that multi-year droughts are expected after 2059, for three investigated
61 springs in Greece under all varying climatic scenarios. Moreover, Hartmann et al., (2012) show
62 that a 10 to 30% decrease in flowrate is expected in a large karst spring in the West Bank after
63 2068. Furthermore, in Lebanon, it is expected under forecasted climatic scenarios (2020-2100;
64 e.g., IPSL_CM5; GCM; RCP, 6.0) to witness a high variability of spring flow rates with more
65 pronounced extremes and periods of droughts (Doummar et al., 2018b) in snow-governed
66 mountainous areas. Additionally, sensitivity studies show the high influence of varying climatic
67 factors (notably precipitation) on spring hydrographs (Dubois et al., 2020, Sivelle et al., 2021)
68 and water availability.

69 Karst springs are an important component of the groundwater systems and play a significant role
70 in the development of civilizations (Luo, et al., 2020, Stevanović 2019b). Particularly, springs
71 have been investigated as vital resources for social and economic development (Andreo et al.,
72 2006, He and Wu., 2019) in many areas around the world, such as Jinan Springs (Gao et al.,
73 2020), Gallusquelle Spring in the Swabian Alps (Sauter 1992, Heinz et al., 2009, Doummar et
74 al., 2012a), and notably around the Mediterranean area (Nerantzaki and Nikolaidis, 2020). In
75 these semi-arid environments where water scarcity is rapidly increasing (Hartmann et al., 2014a),
76 springs have been regarded as important resources for large to small scale local water supply
77 such as El Gran Sasso springs in Italy (Barbieri et al., 2005, Pettita, et al., 2020), the Lez spring
78 in southern France for Montpellier (Fleury et al., 2009, Marechal et al., 2013, Sivelles et al.
79 2021); the Eastern Ronda Springs and Ubrique spring for Malaga Province in Southern Spain
80 (Barbera and Andreo, 2012, Hartmann et al., 2013, Marin et al., 2021). In these areas, the
81 continuous monitoring of spring quality and quantity is performed to ensure sustainability in the
82 supply and the preservation of the water quality at the source. The increasing urbanization,
83 especially in areas that lack waste-water treatment plants (mostly in rural developing countries)
84 has resulted in a growing level of unpredictable contamination (Gao et al., 2020). Furthermore, a
85 sturdy understanding of the hydrological processes and the factors influencing groundwater
86 dynamics including climatic ones are needed to develop well-informed water management tools
87 and policies (Luo et al., 2020, Stevanović and Stevanović, 2021). Numerical models have been
88 proposed as successful decision support tools for water management in karst (Sivelles et al.,
89 2021). Flow in these systems has been simulated using lumped and distributed approaches
90 depending on the level of surface and subsurface characterization (Worthington, 1999,
91 Doummar et al., 2012a, Hartmann et al., 2013b, Duran and Gill, 2021). However, the suitability

92 of the model highly relies on the amount and quality of the available data and its temporal extent
93 (Hartmann et al., 2017). In some instances, robust sensitivity analysis allows decreasing the
94 uncertainty in the model output (Hartmann et al., 2013c, Chen et al., 2014, Mazilli et al., 2017,
95 Dubois et al., 2020). To overcome the challenges of transport assessment in karst, even with a
96 calibrated and validated flow model, the analysis of spring responses provides insights into the
97 dynamics of a karst system. Firstly, the breakthrough of conservative (or reactive) contaminants
98 and/or spring signatures (stable isotopes) have been used in spring high-resolution time series to
99 understand the dynamic response of springs to a variation in input and extent of dilution (Frank
100 et al., 2018, Hillebrand et al., 2015, Wang et al., 2020, Ahmed et al., 2021). Moreover, tracer
101 experiments have been implemented to assess the connection between karst springs and a
102 contamination point source and estimate transport velocities and dispersivity (Goepfert and
103 Goldscheider, 2008, Marin et al., 2015, Doummar et al., 2018a, Benischke, 2021) in the aquifer
104 and its intrinsic vulnerability to contamination (Epting et al., 2018). Additionally, emerging
105 micropollutants (MPs) such as pharmaceuticals and personal care products were revealed to be
106 suitable transport indicators for persistent and degradable contamination of different origins
107 (Hillebrand et al., 2012, Doummar et al., 2014, Zirlewagen et al., 2016, Stange and Tiehm,
108 2020). They can be detected to various extents in raw wastewater and treated wastewater, if
109 persistent, or in groundwater and surface water, notably in areas lacking proper wastewater
110 treatment systems (Gasser et al., 2010, Schmidt et al., 2013, Doummar and Aoun, 2018a,
111 Clemens et al., 2020).

112 Lebanon counts more than 409 springs with discharges ranging between 0.001 m³/s to more than
113 10 m³/s on average (ElGhawi et al., 2021). Some are used for local supply, while others may
114 serve as an alternative decentralized water source for selected villages to overcome the

115 forecasted water scarcity. The high urbanization and lack of an effective wastewater system in
116 Lebanon (Massoud et al., 2010), pose a significant contamination risk on springs located below
117 1600 m above sea level even in rural settings. Therefore, there is a need for thorough
118 investigations on selected potential springs, to understand their vulnerability against
119 contamination events or climatic parameters (Epting et al., 2018). The latter can be only
120 achieved with a robust monitoring network, the collection of high-resolution data, the analysis of
121 representative temporal and spatial water quality samples, and the assessment of contamination
122 indicators (Torresan et al., 2020). The objective of this work is to highlight some of the
123 important methods used for the conceptualization of flow and transport in pilot karst springs and
124 the identification of their inherent resilience to contamination hazards and potential future threats
125 in a rural groundwater catchment in Lebanon. The proposed methodology can be applied to other
126 case studies in poorly investigated spring catchment areas. The results are further discussed in
127 terms of policy enforcement and drafting of guidelines and laws to ensure sustainable protection
128 of spring water resources (Fleury, 2009).

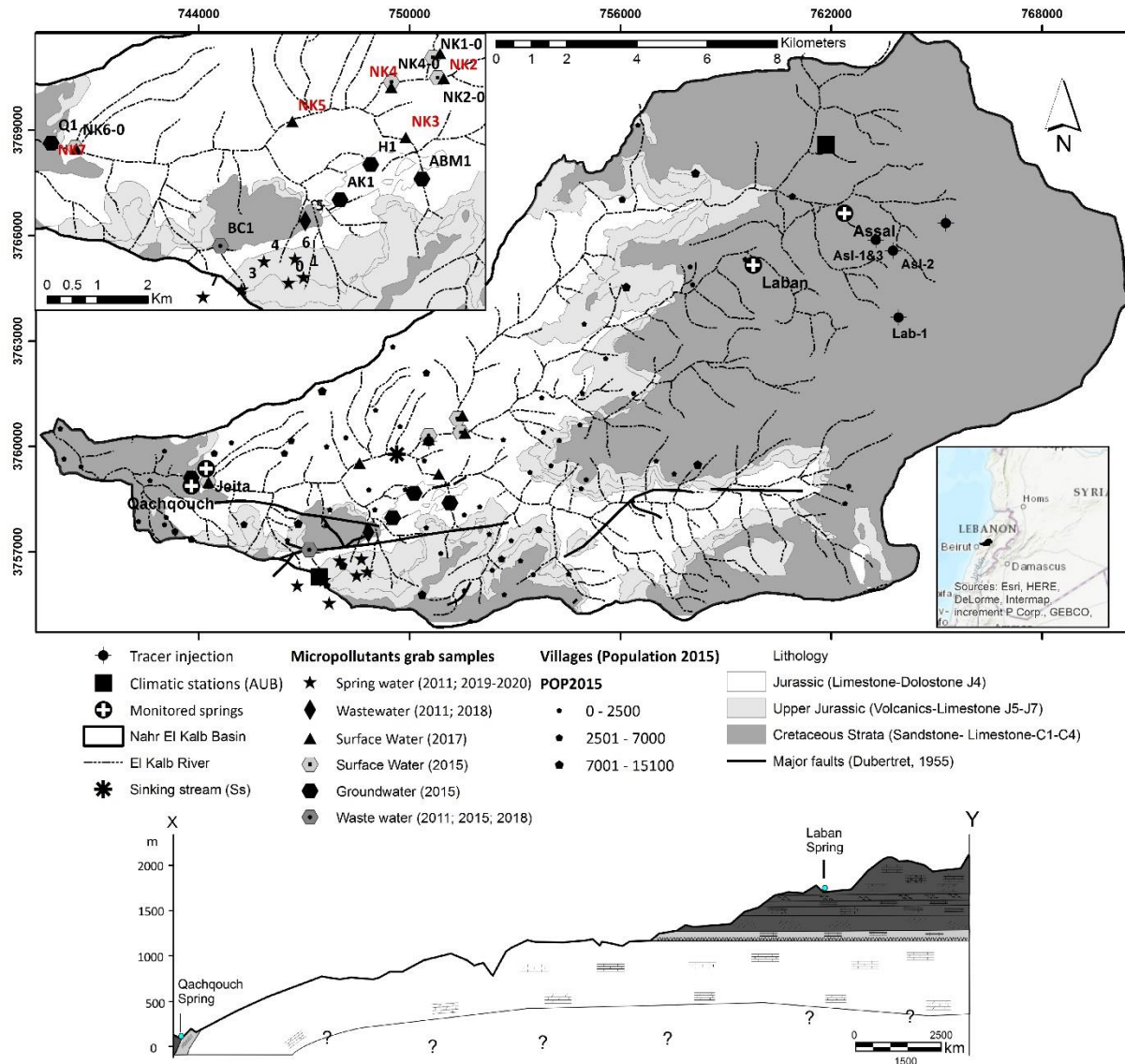
129 **2. Field site**

130 The investigated springs are located in the Middle East- Lebanon, north of the capital Beirut in a
131 Mediterranean semi-arid snow-governed climatic region (Figure 1, Table 1). They belong to the
132 Nahr El Kalb River rural catchment (Figure 1). The catchment extends from sea level to an
133 elevation of 2600 m above sea level and is characterized by karstified Jurassic and Cretaceous
134 rock sequences disturbed by complex structural deformations (Bakalowicz, 2015). The
135 catchment is drained by important springs heavily relied upon for water supply; for instance, the
136 Jeita spring with mean flowrates of 8 m³/s is used as a water supply source for the capital Beirut
137 (1.5 million inhabitants; Doummar et al., 2014, Koeniger et al., 2017).

138 Based on two recording stations, the total precipitation recorded on the catchment area varies
139 between 800 mm (closer to the coast) and 1800 mm as snow in the mountains (Fayad et al.,
140 2017; Koeniger et al., 2017, Doummar et al., 2018b, Dubois et al., 2020). The Qachqouch Spring
141 located at 64 m above sea level, emerges from Jurassic age rocks, composed of fractured
142 limestone and basalts. During low flow periods, the spring is used to complement the water
143 deficit in the capital city Beirut and surrounding areas. Its total yearly discharge reaches 35-55
144 Mm³ based on high-resolution monitoring of the spring (2014-ongoing; Dubois et al., 2020).
145 Flow maxima reach a value of 10 m³/s for short periods following flood events; it is about 2 m³/s
146 during high flow periods and 0.2 m³/s during recession periods. On the other hand, Laban and
147 Assal Springs are located in the highlands of Nahr El Kalb catchment, at respective altitudes of
148 1552 and 1600 m above sea level. The main source of recharge is the snowmelt over a total
149 groundwater basin of about 25 km². They partially drain the Albian-Cenomanian rock formations
150 composed of limestone and dolostones. The upper catchment area is a plateau characterized by a
151 high-density doline distribution (exceeding 19 dolines/km²), which enable relatively fast
152 infiltration of snowmelt and rain. The dolines mapped during various campaigns (2012, by the
153 BGR: BundesAnstalt Fuer Geowissenschaften and Rohstoffe; by AUB 2015 and AUB 2020-21
154 are buried ones with non- discernable 20-50 cm swallets buried by rock debris. Fast infiltration
155 of rain or snowmelt can occur in the buried holes within the doline while diffuse infiltration
156 happens within the soil depending on the rock facies in the Cenomanian rock sequence. The
157 thickness of the soil in the dolines may exceed 5 m as portrayed by representative auger
158 excavations. The Assal spring has an annual volume of 22-30 Mm³ (Doummar et al., 2018b) is
159 used locally for water supply 24,000 m³/day while water from the Laban spring, with a total
160 annual volume of 20-25 Mm³, is conveyed to the Chabrouh Dam in Faraya (Figure 1). The

161 overflow from both springs feeds the two tributaries of the Dog River (Nahr El Kalb) in the
162 highlands (Doummar and Aoun 2018a), while that of Qachqouch spring is discharged into the
163 River closer to the coast. The highest observed volumes in the three springs are recorded during
164 the high flow periods (December to April) exceed the water demand and supply, while available
165 water volumes drop substantially during low flow periods extending from May till November
166 where water supply is mostly needed. Therefore the three karst springs are currently not
167 exploited to their full potential, due to the presence of alternative resources and the natural deficit
168 in water availability during low flow owing to their karstic nature. The Qachqouch spring is a
169 karst spring characterized by a duality of flow in a low permeability matrix and high
170 permeability phreatic conduit system (Dubois et al., 2020). As such, it is highly reactive to rain
171 events with a recession coefficient ranging between 0.005 and 0.1 depending on the event
172 responses (Dubois et al., 2020). Assal spring is less responsive to snowmelt and is characterized
173 by a storage capacity that allows it to sustain a flow rate of 240 l/s during the dry season (August
174 till October). The Laban spring is highly reactive to snowmelt due to its higher level of
175 karstification and has a limited storage capacity, thus it runs almost dry during the summer
176 period (August-October). Wastewater treatment plants are absent in most areas in Lebanon,
177 especially in rural areas because of the difficulty of continuous operation and maintenance
178 (Karnib, 2014). Additionally, wastewater effluents and solid waste may be disposed of directly
179 on the river flanks, or in bottomless septic tanks in areas that are not connected to the public
180 wastewater network (Massoud et al., 2010). Furthermore, outdated generic groundwater
181 protection guidelines or laws (for wells, springs, and River) are not reinforced or rigorous
182 enough to ensure the protection of spring catchment areas. As a consequence, land use and cover
183 expand in highly vulnerable areas of spring recharge without proper mitigation measures (Korfali

184 and Jurdi, 2009). The major threats faced by the investigated springs are related to intrinsic or
185 anthropogenic factors influencing both the pristine spring water quality and quantity yielding an
186 increase in the karst disturbance factor (van Beynen and Townsend, 2005, North et al., 2009).
187 Such threats can decrease the available water of good quality for supply over the short- and long-
188 term scale (especially in countries that have adhered to the United Nations Sustainable
189 Developmental goals (SDG VI). On the other hand, the opportunities are infrastructural,
190 technological, or policy-making changes that can enhance the sustainable supply of water
191 quantity over time, mitigate the contamination risk, and achieve a potential recovery of the
192 pristine status of the spring.



193

194 Figure 1. Geological map showing the location of the three investigated springs and the
 195 location of collected samples on the Nahr El Kalb Catchment. A conceptual cross section shows
 196 the different lithologies and thicknesses of the main aquifers

197 Table 1 Geological and hydrogeological characteristics of the three investigated springs

Spring	X Y Z (m above sea level) (WGS, 1984)	Formation	Major threats	Major opportunities
Qachqouch	33.943985°N 35.637690°E 64 m	Jurassic limestone, Aquifer highly	Water contamination from	Floodwaters to be used for managed aquifer recharge or to

Spring	X Y Z (m above sea level) (WGS, 1984)	Formation	Major threats	Major opportunities
		karstified and responsive to rain events (the flow rates increase shortly following precipitation events, Low to moderate storage	waste water effluents surface-water Interaction (Doummar ad Aoun, 2018 a, b)	compensate for the water shortage
Assal	34.009710° N 35.838760°E 1552 m	Cenomanian dolostones and limestone, medium karstified high storage capacity, Reactive to snowmelt events	Increasing waste water contamination Climate change, snow cover decrease, longer recession period because of earlier snowmelt and	Limited land use/landcover leading to limited contamination Snowmelt ensures a longer-lasting recession, springs can be used to compensate low flow shortages at lower altitudes
Laban	33.994961°N 35.828203°E 1662 m	Cenomanian limestone, Highly karstified, Low storage capacity, Reactive to snowmelt	increasing temperatures (Doummar et al., 2018 b)	

198 **3. Investigation Methods**

199 Extensive hydrogeological studies are performed on spring water, including 1) high-resolution
200 monitoring to analyze flow dynamics and hydro-chemical variations (Gao et al., 2020), 2)
201 Assessment of intrinsic transport from tracer experiments, 3) Evaluation of specific transport of
202 selected micropollutants. These methods aims at collecting sufficient data about water quality
203 and quantity, and at constructing conceptual models that feed into process- based numerical
204 models to be calibrated based on continuous data acquisition and system characterizations. Such

205 models if validated can be used for prediction purposes (Hartmann et al., 2014b, 2020),
 206 ultimately to anticipate the forthcoming threats on existing springs.

207 3.1 High-resolution data collection

208 A rigorous monitoring network in groundwater basins is lacking in Lebanon due to the high cost
 209 of maintenance and operation. Therefore, since 2014, a monitoring network was set up to collect
 210 high-resolution data on a pilot catchment area (in the framework of international research
 211 projects). This constant monitoring of spring flow and quality allows quantifying the water
 212 volumes, the flow rates, and their variation during the hydrological regimes (Mudarra et al.,
 213 2012) and consequently ensure the evidence-supported protection of the investigated springs in
 214 terms of quality and quantity. The collected monitoring data in the three springs and catchment
 215 consists of automatic data, grab samples, and automatic sampling entailing climate and flow
 216 data, as well as physico-chemical data. The rate and frequency of sampling along with the type
 217 of data is directly linked to the information required for spring characterization (Table 2).

218 Table 2 Information provided by the measured parameters/ experiments on springs used
 219 for spring characterization and construction of conceptual models

Spring Parameters and frequency of measurements	Indicator for spring response used as input for conceptual and numerical models	Selected literature
Flow rates/ Water level 2014-ongoing	Time series correlative analysis and statistical correlation between input and output Evaluation of aquifer type, storage, and recession Insights into aquifer geometry Analysis of snow melt on volume and spring dependence of climate variability and change Applications: Water availability and alternatives	Lu and Liu, 2020 Olarinoye et al., 2020 Dubois et al., 2020
Bacteriological analysis, Turbidity and Particle distribution	Indicative of potential bacteriological contamination	Pronk et al., 2006, Stedmon et al., 2011, Frank et al., 2018

Spring Parameters and frequency of measurements	Indicator for spring response used as input for conceptual and numerical models	Selected literature
Periodically 2019-ongoing Occasionally or event based prior to 2019	Application in early warning systems and contamination indicator	
Electrical conductivity Temperature 2014- ongoing	Indicative of fast infiltrated water from point source origin and snow component Degree of karstification	Lu and Liu, 2020 Wang et al., 2020 Torresan et al., 2020, Ahmed et al., 2021
Chemical analysis Periodically 2019-ongoing Occasionally or event based prior to 2019	Insights into water-rock interaction, Identification and estimation of anthropogenic contamination indicator	Gasser et al., 2010 Schmidt et al., 2013
Micropollutants (Pharmaceuticals and Personal Care Products; PPCPs) Occasionally or event based	Origin of contaminants Transport and persistence of compounds in the matrix Type of infiltration (diffuse versus point source) Specific vulnerability	Einsiedl et al., 2010 Doummar et al., 2014 Doummar and Aoun 2018a and b, Warner et al., 2019
Artificial tracer experiments Occasionally or event based. Constant monitoring with field fluorometer	Intrinsic vulnerability Spring protection Contaminant outbreak management	Geyer et al., 2007, Goepfert and Goldscheider, 2008, Doummar et al., 2018a Beniscke et al., 2021
Stable Isotopes (Oxygen and Hydrogen) Since 2019 Occasionally or event based prior to 2019	Recharge assessment (quantification of fast infiltration, elevation etc.)	Perrin et al., 2003 Barbieri et al., 2005 Koeniger et al., 2017 Rusjan et al., 2019

- 220 1. Climatic stations (HOBO and alpine Campbell brands) for the measurement of precipitation
221 (including snow), humidity, wind direction and magnitude, temperature, and radiation at two
222 different altitudes (950 and 1700 m above sea level). The data is used for the assessment of
223 potential evapotranspiration and input precipitation (frequency of 15 -60 min) and snowmelt
224 based on temperature variation.
- 225 2. Flow monitoring in the River and springs is done using pressure transducers for water level
226 measurement. Discharge is estimated using rating curves based on the monthly measurements

227 of discharge. Where and when accessibility to both spring and River is constrained,
228 uncertainties in high flow periods may lead to an overestimation of the annual budget, and
229 consequently the quantities of water available for supply in addition to the calculation of
230 contaminant/tracer masses. The error in flood flowrates can be reduced or quantified based on
231 the analysis of a longer time-series data set due to the high variability and seasonality of flow
232 in addition to a statistical analysis of numerical modelling output. However, these errors are
233 not detrimental to the conceptualization of flow and early numerical modelling calibration.

234 3. In situ physico-chemical parameters are measured with a periodically calibrated (when needed)
235 multi-parameter probe (Aquatroll 600- Insitu) for Electrical Conductivity (EC), Temperature
236 (T), Turbidity (TU), and pH, as well as Dissolved Oxygen (DO) installed on the spring.

237 4. Two automatic samplers are scheduled every 3 days to collect samples for the analysis of
238 indicator parameters in spring water (El Qachqouch) for the following analysis:

239 ▪ Stable Isotopes (Oxygen and Deuterium) collected in glass bottles analysed using a
240 PICARRO isotopic analyzer L2130-i cavity ring-down spectrometer (CRDS) with a VAP
241 A0211 vaporizer and automatic sampler. The standards for oxygen and hydrogen used for
242 calibration and routine checking of the measurements, are well preserved standards of
243 known isotopic composition (values versus VSMOW for $\delta^{18}\text{O}$: 0.3, -20.6, -29.6 ‰, and for
244 $\delta^2\text{H}$: 1.8, -159, and -235.0 ‰,)

245 ▪ Major ions for water types and pollution assessment collected occasionally to weekly
246 analyzed using Ion Chromatography (IC) with the appropriate concentration standards for
247 the respective measured ions.

248 ▪ Particle size distribution for the assessment of suspended particles leading to turbidity
249 using a Coulter counter (Multi-sizer 4e, Brand Beckman) with different apertures used
250 according to the grain size measurements (ranging from 2µm- 2000 µm)

251 5. Field fluorometers (GGUN-FL30-Albilis) are installed at each spring for the measurements of
252 natural fluorescence in pristine waters and tracer experiments conducted on injection points on
253 the catchment area. The fluorometers were calibrated in the field following each experiments
254 with the injected tracer and the spring water.

255 6. Bacteriological analysis (*fecal and total coliform, pseudomonas aeruginosa and enterococci*)
256 analyzed occasionally) at a local certified bacteriological laboratory to detect the variation of
257 fecal indicators in the spring and associate it with continuous point-source contamination on
258 the catchment.

259 3.2 Tracer experiments and identification of transport parameters

260 3.2.1 Tracer experiments

261 Tracer experiments were undertaken on the catchment area, whereby artificial dyes
262 (uranine; sodium fluorescein and occasionally amidorhodamine-G), considered
263 conservative and nontoxic to humans and the environment (Käss, 1998) were injected in
264 the River (Qachqouch catchment) and specific dolines on the catchment of the Laban and
265 Assal springs. Tracer concentrations were simultaneously monitored and recorded every 15
266 min in the spring using a field fluorometer (GGUN-FL30; Schnegg, 2002) that was
267 calibrated for the applied tracers. Discharge measurements were estimated based on the
268 recorded water level and rating curve under different flow conditions (high flow, low flow,
269 snowmelt, and medium flow). Restitution of the tracer allows identifying a connection

270 between the injection point, considered as a vulnerable contribution point of the recharge
271 area, and the spring (Benischke, 2021). Furthermore, the transport parameters such as
272 mean velocity and dispersivity can be estimated for conservative pollutants based on the
273 analysis of the breakthrough curve using a 1-D transport model (Toride et al., 1999; Geyer
274 et al. 2007, Goeppert et al. 2020, Sivelle et al., 2020). Tracer experiments reflect the
275 intrinsic vulnerability of a spring system as well as the transport mechanisms of a
276 conservative pollutant from different origins (fast preferential flow; doline, or a sinking
277 allochthonous stream; River). While the duration of tracer recovery provides insights into
278 the duration of the breakthrough of a non-reactive pollutant, the observed tracer
279 concentration is indicative of the intensity of the contamination above admissible limits for
280 a certain contaminant load (Doummar et al., 2018a).

281 3.2.2 Micropollutant analysis

282 Micropollutants (MPs) were analyzed in 75 grab samples collected from surface water,
283 wastewater, wells, and springs in 2015-2019 to characterize the point source contaminants
284 existing on the catchment area. Additional limited samples collected and analyzed in 2011
285 (Doummar et al., 2012b) serve for comparison purposes of the variation of MPs over the last
286 decade. The selected micropollutants span from pharmaceuticals to personal care products
287 present in domestic, industrial, and hospital wastewater effluents such as nonsteroidal anti-
288 inflammatory drug (ibuprofen), lipid regulators (gemfibrozil), artificial sweeteners (sucralose,
289 and acesulfame-K), epileptic drugs (carbamazepine), bronchodilators (albuterol), hospital
290 contrast media (iohexol), detergents (nonylphenol), dyes manufacturing (quinoline) and others
291 (metformin, and caffeine). Furthermore, these pharmaceuticals were also monitored in one of the
292 springs to detect the variations in concentrations and loads in spring water (Zuccato et al., 2005,

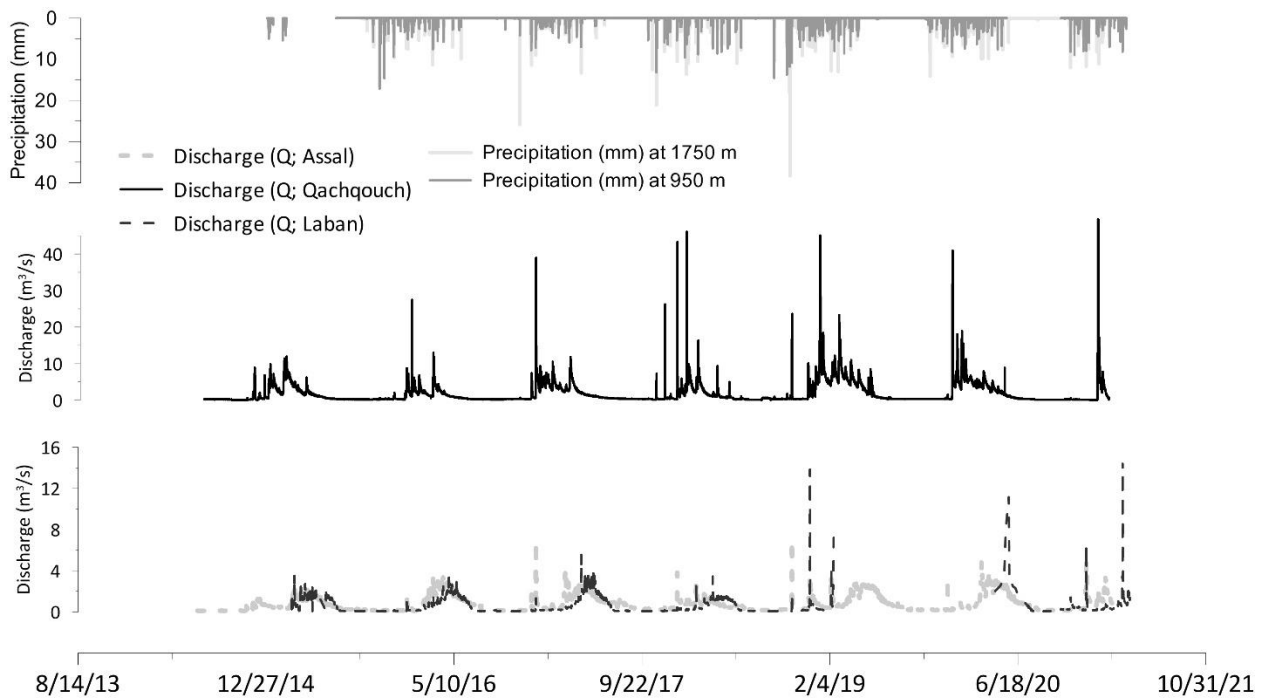
293 Hillebrand et al., 2012). Moreover, the breakthrough of MPs loads and concentrations in the
294 spring was related to the origin of effluents (surface water or point source infiltration) according
295 to the flow dynamics based on binary mixing models (Buerge et al, 2009, Gasser et al., 2010,
296 Doummar et al., 2014, Mawhinney et al, 2011, Oppenheimer et al, 2011, Wolf et al, 2012, van
297 Stempvoort et al, 2013, Liu et al, 2014, Nödler et al, 2016). The MPs that are revealed to be
298 persistent and least degradable in the system independent of recharge are the ones that can be
299 used as viable wastewater indicators (Oppenheimer et. Al., 2011) and can be of threat to the
300 spring water quality if they exceed the maximum admissible limits (MAL). Additionally, the
301 distribution and evolution of MPs concentrations can provide insights into the type of wastewater
302 and water usage on the rural catchment (Werner et al., 2019).

303 A correlation between easily monitored parameters at the spring, for example, turbidity and
304 electrical conductivity with the breakthrough of these emerging micropollutants such as
305 Ibuprofen, sucralose and acesulfame-K, and carbamazepine), gemfibrozil was used to assess the
306 contamination arrival at the spring with easily measured indicator parameters (Doummar et al.,
307 2018b). Binary and ternary mixing models (based on mass-fluxes of chloride, micropollutants,
308 and stable isotopes) are used to identify the percentage of wastewater inflow into pristine
309 groundwater (from wastewater effluents discarded on the catchment and in the River; Gasser et
310 al., 2010, Schmidt et al., 2013, Doummar and Aoun 2018a). The analysis of the breakthrough
311 curve of micropollutants with other measured parameters (electrical conductivity, chloride and
312 calcium, etc.) allows identifying mass fluxes of these persistent pharmaceuticals (Doummar et
313 al., 2014, Doummar and Aoun, 2018b).

314 **4. Discussion and results**

315 4.1 High-resolution data as insight to systems hydrodynamics

316 The high-resolution data (until 2018) from the three existing springs was partially included in the
317 global data set on karst springs (Olarinoye et al., 2020). The three springs shows an uneven
318 distribution of flowrates during the year indicating a shortage in the summer time following the
319 hydrograph recession. The total water volumes throughout the six years show a high variability
320 from dry to intermediate to wet years, typical of semi-arid regions, which adds to the lack of
321 predictability in water availability for supply (Figure 2, Table 3). The Qachqouch spring is
322 characterized by flood waters that can reach up to 50 Mm³ during high flow periods in wet years
323 (the discharge rates exceeding its average discharge during low flow periods as recorded in July-
324 October).



325

326 Figure 2 Spring hydrographs for the three monitored springs illustrating the variation in
327 discharge for along with total amount of precipitation (snow and rain)

328 Table 3 Spring volumes illustrating the variation from wet (2018-2020), intermediate
 329 (2016-2017) and dry years (2014-2017 and 207-2018). Spring type and coefficient estimated
 330 from spring hydrographs.

	2014-15	2015-16	2016-17	2017-18	2018-19	2019-20	Spring type *(k, i)
Precipitation (950 m)	NA	921.6	1034	1090	1764	1319	
Precipitation (1700 m)	NA	1110	1005	1084	1838	1405	
V Qachqouch (Mm ³)	49.80	35.80	61.50	43.40	100.1	69.20	**Type 1 (0.11, 0.77)
V Laban (Mm ³)	NA	16.10	18.90	12.50	NA	20.00	***Type 2 (0.09, 0.24)
V Assal (Mm ³)	NA	24.20	24.60	16.90	30.90	27.10	***Type 3 (0.4, 0.44)

*After Mangin, 1975; k: characterizes the extent of the phreatic zone and its regulating capacity; its storage and discharge of fast infiltrated water ($k > 0.5$ is characteristic of porous aquifer), i close to 0 implies a fast infiltration, compared to a value closer to 1.

**from Dubois et al., 2020

*** Calculated based on time series following the method by Mangin, 1975 in Dubois et al., 2020

331 Detailed correlative analysis of time series reveals information about the geometry and the
 332 parametrization of a subsurface karst system (Mangin, 1975, Dubois et al., 2020,). For instance,
 333 the number of groundwater reservoirs and the spring recession coefficients are inferred from
 334 statistical analysis of time series (discharge, electrical conductivity, precipitation). Furthermore,
 335 the analysis of the flow time series can yield a classification of the spring typology (Mangin,
 336 1975, El Hakim et al., 2007, Stevanovic, 2015), which unravel the type of flow, indicative of the
 337 behavioral response of the spring, its reactivity versus storage capacity, and its porosity type
 338 (equivalent porous, versus dual and triple porosity). Additionally, the springs response (discharge
 339 and other monitored parameters) to rain or snowmelt events provides valuable information about
 340 the total volume of fast point source infiltration (such as dolines). In the Qachqouch spring, the
 341 correlation of electrical conductivity, stable isotopes, and chloride along with flow show that the
 342 newly recharged water range between 10 and 70 % of the total volume per event. The latter

343 being highly dependent on the saturation of the system. On the other hand, the Assal spring is
344 classified as type 3, characterized by a slow infiltration and a higher storage. The discharge curve
345 displays a fluctuation indicative of diurnal snowmelt and nocturnal freezing. The volume of
346 freshly infiltrated snowmelt directly related to the number of dolines on the catchment is also
347 estimated daily based on the high-resolution data series. The relevance of newly infiltrated water
348 or snow has an important implication if it is closely related to a point source contamination
349 (Jodar et al., 2020). On the other hand, the Laban spring located 2 km away from El Assal
350 spring within the same aquifer, displays a different hydrodynamic behavior, as shown from a k
351 value closer to 1, and an I value closer to 0. The latter can be attributed to the variation of facies
352 within the Cenomanian aquifer (lower dolomitic member versus the upper more karstified
353 limestone member).

354 4.2 Assessment of spring intrinsic vulnerability

355 4.2.1 Qachqouch Spring

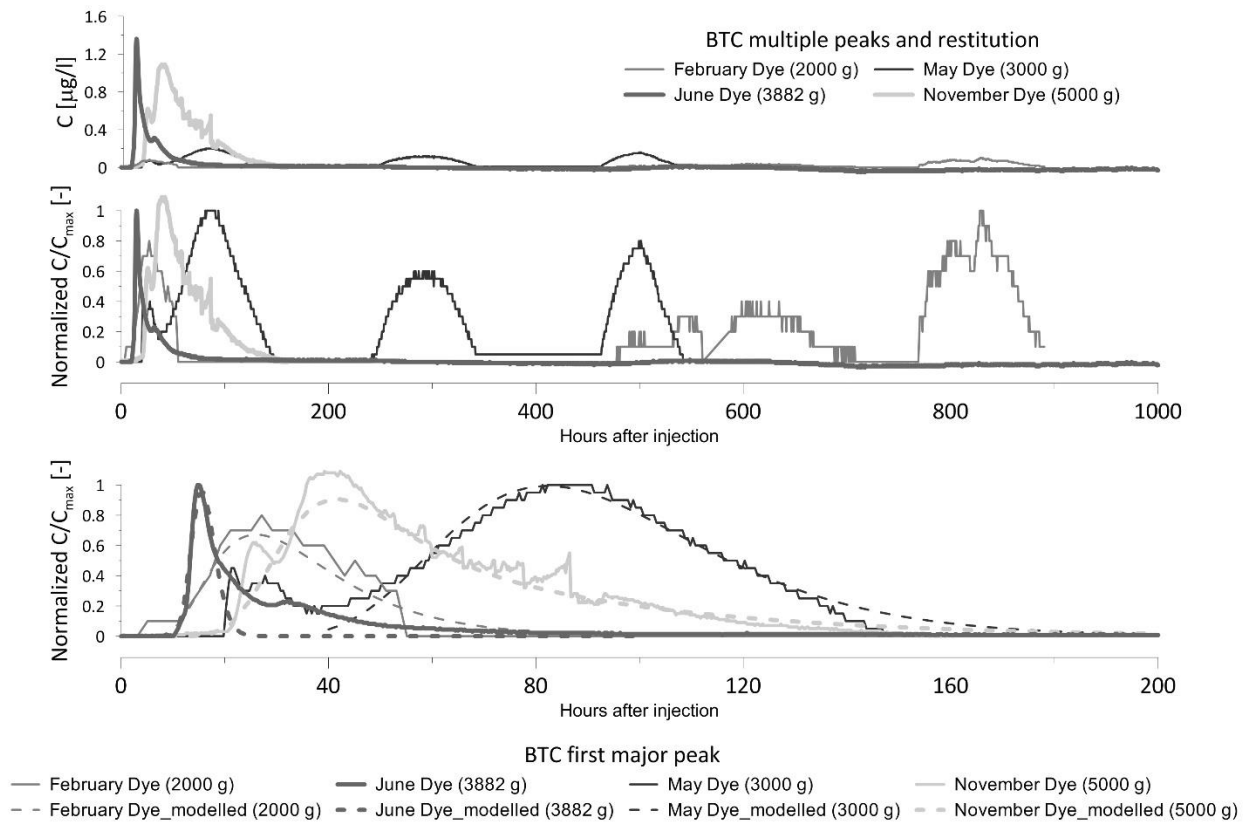
356 The tracer breakthrough curve (BTC) recorded at the Qachqouch spring reveals a connection
357 between the River and the spring (Figure 3, Table 4). the breakthrough curve was characterized
358 by one main peak and other minor peaks or discontinuous recovery of the tracer for a longer
359 period. The first peak in May and November dyes appear as a composite peak, which may be
360 due to a considerable longitudinal dispersion in the River before infiltration occurs during snow
361 melt and low flow periods. The injected uranine was first detected at the spring between 5 to 20
362 hours after injection, which corresponds to maximum transport velocities of 0.07 m/s, 0.17 m/s,
363 0.25 m/s, and 0.77 m/s in, May, November, June, and February respectively (Figure 3). The
364 mean velocities and dispersivities are estimated for the first main peak of the BTC based on 1-D

365 analytical solutions for transport Two-Region Non-equilibrium model (2NREM) depending on
 366 the extent of tailing and shape of the BTC (Figure 3).

367 Table 4 Characteristics of the tracer experiments, results of the graphical interpretation
 368 and estimation of transport parameters based on BTC analysis and inverse modeling

Name		May Dye			Feb Dye			Novem-ber Dye	June Dye	Asl-1	Asl-2	Asl-3	Lab-1
Injection points		Sinking stream (Nahr El Kalb)							Doline			Doline	
Observation point		Qachqouch spring							Assal			Laban	
Date		05/08/16			02/19/17			11/24/17	06/04/20	07/01/14	06/01/16	05/01/15	07/01/20
Type of BTC		Multi peak (3 peaks)			Multi peak (3 peaks)			One major peak					
Tracer type		SF			AR			SF	SF	SF	SF	AR	SF
M	g	3000			2000			5000	3883	400	2000	1500	2408
x	m	8920			8700			8920	8920	1330	2330	1330	3140
M _R	g	71			150			58	213	112	360	135	241
M _R	%	2%			8%			1%	5%	28%	18%	9%	10%
Break-through peaks (P)		P1	P2	P3	P1	P2	P3	P1	P1	P1	P1	P1	P1
Q _{mean}	m ³ /s	0.78	0.65	0.62	4.86	3.16	3.98	0.37	0.72	0.25	0.31	1.05	0.27
C _p	[µg/l]	0.2	0.12	0.16	0.09	0.03	0.04	1.07	1.36	1.5	2	0.9	5
T _f	[h]	35	242	461	3	480	768	15	10	288.0	175.2	21.0	65.4
t _{cp}	[h]	87	293	500	22	604	829	42	15	336.0	197.0	29.0	87.0
v _f	m/h	255	37	19	2788	18	11	595	893	4.62	13.30	63.30	48.00
v _f	m/s	0.07	0.01	0.01	0.77	0.01	0.00	0.17	0.25	0.0013	0.0037	0.0176	0.0133
Duration BTC	hours	112	233	81	55	226	121	156	110	182	71	>220	535
	days	4.68	9.73	3.36	2.29	9.42	5.04	6.50	4.58	8	2.95	>10	22.3
Model		2NRE			2RNE			2RNE	2RNE	AD	AD	AD	AD
v _m	[m/h]	66			241			140	421	3.8	11.4	45.7	34.4
v _m	[m/s]	0.018			0.067			0.039	0.117	0.001	0.003	0.013	0.010
D _m	[m ² /h]	27000			188000			50000	16600	24	79	300	458
D	[m ² /s]	8			NA			14	5	0.007	0.022	0.083	0.127
t _m	[h]	135			36			64	21	1.40	7.38	16.88	30.00
α	[m]	408			780			357	39	6.32	6.89	6.56	13.31
φ	m	3.66			4.80			1.74	1.40	0.55	1.10	3.91	1.71

369
 370 The dispersivities ranging between 39 and 780 m are indicative of transport in karst (Doummar
 371 et al., 2018a) and imply the duration of recovery of a tracer and a potential conservative
 372 contaminant from the River.



373

374 Figure 3 Tracer breakthrough curves (BTC) recorded at Qachqouch springs from four
 375 injections in the Nahr El Kalb sinking stream (2016-2020). First peaks in the BTCs are modelled
 376 using 2NRE model to account for the tailing effect.

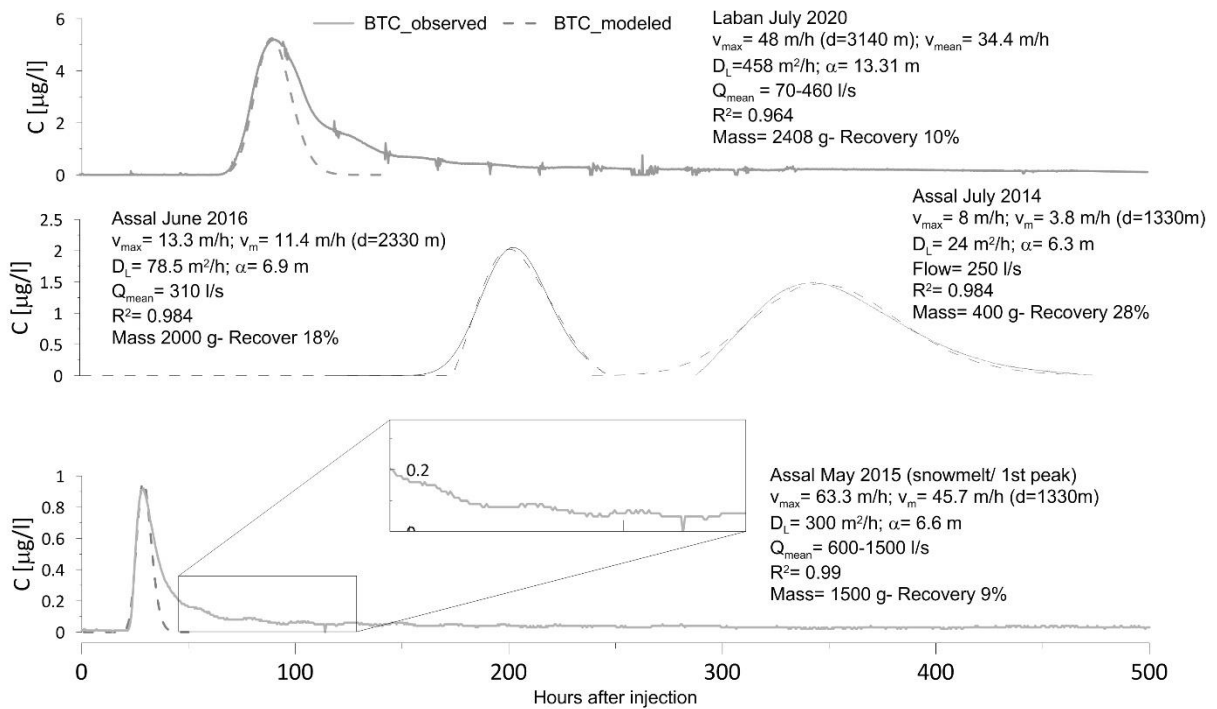
377 The tracer experiment indicates a relationship between the heavily polluted River and the spring
 378 under different flow conditions. During high flow conditions, as the base level in the River is
 379 higher, infiltration through fast flow pathways along the river (sinking streams and karst
 380 flooding) is more prominent (Gutierrez et al., 2014), as indicated by the higher mass recovery
 381 during February (8% compared to 1 % during the lowest flow). Despite a highest infiltration of
 382 River water in the spring during February, the dilution attenuates the maximum concentration of
 383 the BTC. On the other hand, in November, the observed concentrations of conservative
 384 contaminants are expected to be highest despite the limited mass loads from the River. The first
 385 peak in the BTC recovered in the Qachqouch lasts between 2.5-6.5 days, while the tracer
 386 continues to appear in the spring for more than 40 days. The duration and number of peaks

387 depend on the tracer injection and mass, as well as on the flow regimes in both the River and the
388 spring. On the one hand, the relatively long duration of breakthrough indicates the lingering
389 effect of a contaminant transport between the River and the spring (Figure 3). The multi-peak
390 BTC shows that the River and the Spring are linked by continuous infiltration or through
391 multiple conduits or multiple sinking streams. On the other hand, phreatic diameters calculated
392 based on the total volume of water during the mean transit time of the first BTC peak provide
393 information about the subsurface conduit dimensions and revealed to range between 1.4 and 4.8
394 m under varying flow periods (Table 4). Moreover, the subsurface complexity and heterogeneity
395 can be further assessed with a more advanced modeling of the multiple-peak BTC using a
396 convolution of a multiple-step input breakthrough curves (Siirila-Woodburn et al., 2015).

397 4.2.2 Upper Catchment springs

398 Springs located above 1500 m, namely Laban and Assal springs, are mostly governed by
399 snowmelt and show a high vulnerability both in terms of quantity and quality. The mean
400 transport velocities in Assal range between 0.001 and 0.003 m/s during low flow periods (Figure
401 4). The BTCs recorded at the Assal and Laban springs during a snowmelt event (May 2015 and
402 July 2020 respectively) were modeled using a simple advection dispersion model (ADM), since
403 the tailing effect is due to a superposition of various melting signals. A more advanced model is
404 being implemented to illustrate the convolved tracer arrival with subsequent melting events.
405 Since the tailing was not prominent in the BTCs recorded in low flow periods (June 2014 and
406 2016) are also modeled using the ADM for comparison purposes among tracer results. Tracer
407 experiments undertaken under snow melt conditions in both spring catchments reveals velocities
408 of 0.01-0.013 m/s, indicating a fast response during snow melt. The tracer experiment
409 breakthrough curve is restituted for a duration exceeding 500 hours (or 21 days), because of the

410 reactivation of the tracer in the saturated zone during daily snow melt events, therefore any
 411 conservative contamination occurring at the catchment areas in the investigated dolines will
 412 result in a relatively long breakthrough at the spring, which will require subsequent treatment if
 413 the catchment area is not well protected. Moreover, the melting of the snow highly affects the
 414 discharge at the spring, therefore these springs can be considered highly vulnerable to climate
 415 variability, as they are highly responsive to daily snowmelt events. Longitudinal dispersivities
 416 for both Laban and Assal systems calculated based on longitudinal dispersion and mean
 417 velocities are 6.5 m and 13.3 m, respectively (Table 4). Phreatic diameters between injection
 418 points and springs range between 0.55-3.91 m for Assal spring and 1.71 m for Laban spring
 419 depending on the flow period.



420

421 Figure 4 Tracer breakthrough curves (BTC) recorded at Assal and Laban springs from four
 422 injections in dolines on their respective catchment areas (2014-2020).

423 4.3 Assessment of spring specific vulnerability

424 The concentrations of pharmaceuticals in the springs were below toxic limits in the range of
425 nanograms per liters (Chiffre et al., 2016, Doummar et al., 2018 a and b). Even if not considered
426 of a great threat to human consumption, the identified micropollutants can serve as an indicator
427 for the different type of pollution on the catchment area and of the vulnerability of the springs
428 depending on their source of recharge, and their hydrodynamic characteristics (Werner et al.,
429 2019). On the one hand, three types of pollution sources were identified on the catchment of each
430 spring, the predominant one being related to domestic wastewater effluents (Caffeine, diclofenac,
431 gemfibrozil, artificial sweeteners, carbamazepine, Cotinine). Minor ones related to industrial
432 (Quinoline), hospital (Iohexol), or agricultural practices were also detected, where lipid
433 regulators are used in poultry farms (Doummar and Aoun, 2018a) on the Qachqouch catchment.
434 On the other hand, the raw wastewater collected on the catchment show a similar composition, to
435 the exception of Quinoline used in rural industrial zones (BIK sample). Table 5 displays the
436 range of concentrations for different MPs. The MPs found in the Qachqouch spring water
437 samples are infiltrating via various pathways 1) surface water infiltration, 2) fast infiltration point
438 source such as doline, as well as 3) diffuse infiltration (Doummar and Aoun, 2018b). The most
439 persistent are the ones that are found in the spring during periods where the River is dry and no
440 recharge occurs, such as Carbamazepine and Gemfibrozil. Therefore, these two micropollutants
441 can be used as waste water indicators (Doummar et al., 2014). Mass loads of MPs estimated
442 from flow rates and concentrations allow the backtrack calculations of used drugs and number of
443 users and loads of wastewater on the catchment (Zuccato et al., 2005 for cocaine). For instance,
444 daily mass loads of carbamazepine (CBZ) used on a smaller sub-catchment (small scale springs
445 including three villages) vary between 0.26 and 81 mg/l, while this load increases to 63-5075

446 mg/l per day in the Qachqouch spring because of the inflow of additional point source
447 contamination infiltrating to the spring from the entire catchment.

448 In the upper springs, only caffeine was detected, implying a rather limited amount of
449 contamination due to the lack of urbanization in the highlands of the area (two mountain huts,
450 restricted settlements mostly above Laban spring, and the ski resort). Additionally, the *fecal*
451 *coliform and enterococci* are also limited (Assal: 0-12 CFU/100ml and 0-130 CFU/100 ml), in
452 samples collected during baseflow (July 2020- February 2021) depending on the sampling time,
453 and show a lower level of fecal contamination in the Upper catchment springs. However, it is
454 expected that breakthrough of contaminants occurs from wastewater stored in bottomless pits
455 from mountain huts. The latter require further high-resolution monitoring and tracer experiments
456 in specific locations to test the contribution of such point-sources of pollution.

457 Table 5 Concentrations of micropollutants (ng/l) and bacteriological analysis in surface
458 water, spring, well, and wastewater samples collected on the Nahr El Kalb catchment

Type of sample	Surface water					Groundwater (Springs and wells)							Upper catchment springs				Waste water			
Name	Nahr El Kalb					Spring Qachqouch							Other springs		Wells		Laban	Assal	BC1	BIK
Approximate discharge range (l/s)	NA	NA	250-1810	1097-4800	2000	NA	NA	700	300-7500	290	0.14-1.06	NA	NA				0.1-2			
Bacteriological analysis																				
Date (Bacteriological)	November 2019-Feb 2021					November 2019-Feb 2021							Apr-17	July 2020- February 2021						
Number of samples	12					13							7	5		6		NA		
Fecal coliform (CFU/100ml)	4303-100000					102-3783							3-80	2-500		0-40		NA		
Total Coliform (CFU/100ml)	1686-9799					0-968							NA	0-130		0-12		NA		
Enterococci (CFU/100ml)	450-2500					6-255							NA	0-33		0-3		NA		
Micropollutant analysis																				
Date (Mps)	3/1	9/1	5/1	4/1	6/1	3/1	9/1	5/1	1/1	6/20	4/1	5/1	3/1	9/1	3/1	9/1	3/1	5/1	4/1	
Number of samples (81)	5	1	4	7	3	1	1	1	20	19	7	2	2	1	2	2	1	1	1	
Gemfibrozil (lipid regulators)	21	-	17	47	NA	-	4.6	0	5.2-38	NA	NA	0	-	-	-	-	1424	3500	780	
Iohexal (contrast Media)	-	-	10	33	NA	-	-	12	19-47	NA	NA	0-13	-	-	-	-	-	290	0	
Acesulfame-K (Artificial sweetener)	NA	NA	85	80	NA	NA	NA	170	s	NA	NA	180-640	-	-	-	-	-	210000	10000	
Ibuprofen (nonsteroidal anti-inflammatory drug)	24	-	13	64	NA	-	-	-	-	NA	NA	0	-	-	-	-	>7500	2100	3000	
Diclofenac (Analgesic)	-	-	7	5	NA	-	-	-	-	NA	-	0	-	-	-	-	45	-	310	
Caffeine (Stimulants)	297	190	304	330	22-120	17	9.9	-	-	15-54	14-380	-	6.0	10	0	246	>17000	-	81000	
Cotinine (nicotine metabolite)	16	-	23	47	20-23	-	-	-	NA	-	-	-	-	-	-	-	-	1255	7100	1900
Carbamazepine (Anticonvulsants)	5	25	NA	8	8.1-15	13	43	16.0	NA	16-38	11-890	-	-	-	-	-	227	370	710	
Metformin (Blood sugar control)	NA	NA	NA	NA	NA	NA	NA	NA	NA	-	6-11	NA	-	-	-	-	-	NA	360	
Quinoline (manufacturing dyes)	NA	NA	14	-	NA	NA	NA	-	NA	-	7.6-12	-	-	-	-	-	-	-	330	
Atenolol (Antihypertensive agent)	10	-	6	13	-	-	-	-	0.0	-	19	-	-	-	-	-	0	0	500	
A value of - implies BMRL= Below Mean Reporting Limit																				
NA = not analyzed																				

459

460 4.4 From conceptual to numerical models

461 Conceptual and process-based numerical models are developed based on the synthesis of field
462 experiments and statistical correlative analysis of the time series collected on the spring
463 catchment areas (Mudarra et al., 2019, Dubois et al., 2020). Additionally, insights into the
464 intrinsic and specific vulnerability allow for understanding the recharge mechanisms and point
465 source potential pollution. First, a semi-distributed linear reservoir numerical model has been
466 parameterized and constructed for the complex catchment of Qachqouch spring and further
467 calibrated based on the continuous analysis of field and time-series data (Dubois et al., 2020). a
468 lumped model was selected for the Qachqouch Spring catchment, following the detailed
469 statistical and correlative time- series analysis and spring classification as complex Jurassic

470 highly karstified aquifer. Such high variability of flow and response to rain events, and karst
471 heterogeneity, complex dynamics could not be simulated using an equivalent porous medium
472 continuum model. On the other hand, , a integrated distributed process-based flow model (DFM)
473 was constructed with Mike she (DHI, 2017) for the less karstified Cenomanian aquifer of El
474 Assal spring (using an equivalent porous approach with a bypass function along dolines for fast
475 infiltration; Doummar et al., 2018b). Similarly, a 2-D variable saturated flow (VSF) model was
476 developed by Koohbor et al., (2020) to simulate flow in El Assal spring while accounting for
477 discrete fractures. Both models were used to simulate future flowrates to forecasted climate
478 change scenarios and show a drastic change in water availability after 2070 and a high variability
479 between wet, dry, and intermediate years after 2030 with a steady increase of recession duration
480 of 5.5 days per decade. The VSF model shows that neglecting the fractures leads to an
481 overestimation of the flow. However, the integrated distributed model (DFM) can still serve in
482 the case of El Assal spring to simulate peak and recession flow and help in the understanding of
483 spring response to snow-melt for future management purposes. Furthermore, these models allow
484 to quantify the water availability for supply with some degree of uncertainties based on predicted
485 future flow under various climate conditions and identify water resources alternatives (Hartmann
486 et al., 2012, Doummar et al., 2018b, Sivelle et al., 2021). The results have shown a highest
487 sensitivity of the model output (mean and minimum discharge) to temperature in the snow-
488 governed springs, while a decreasing precipitation will mostly impact the availability of flood
489 waters in the Qachqouch spring at lower elevation. While, these numerical models can be further
490 validated and potentially upscaled to aquifers of similar reservoir characteristics, with a
491 collection of additional data, they can act as a decision support tool to test the response and
492 sensitivity of the springs to a variation in input (temperature, rain, snowmelt) or contamination

493 (Kresic and Stevanović, 2010, Parise et al., 2015). Nonetheless, the selection of the most suitable
494 model depends not only on the type and available data, but also on the degree of heterogeneity of
495 the system and on the model's efficiency of portraying complex karst processes (Scanlon et al.,
496 2003). To overcome this challenge and select the proper modelling approach (lumped,
497 distributed, semi distributed models), it is primordial to achieve a quantitative conceptualization
498 of the karst system in space and time based on a proper long-term hydrogeological assessment
499 and monitoring.

500 **5. Conclusions**

501 This work illustrates a selection of methods used in karst catchments for the proper
502 characterization of spring systems in poorly studied semi-arid regions facing a high risk of water
503 scarcity and pollution. On the one hand, the characterization of flow and transport in these pilot
504 springs allows gathering scientific evidence to support changes in policy and for the
505 establishment of guidelines for the protection of the sustainable quantity and quality of these
506 valuable resources (Fleury, 2013; Parise et al., 2018). For instance, the relationship established
507 from tracer experiments between the River and the spring and the occurrence of indicator
508 micropollutants implies the need for the protection of the El Kalb River against pollution and
509 potential contamination from point source domestic, industrial, and hospital wastewater
510 effluents. Additionally, the groundwater catchment is also characterized by point source
511 contamination as portrayed by the persistent pharmaceuticals detected in the sampled upstream
512 springs and wells. On the other hand, the response of the spring to contamination is not
513 homogenous throughout the year, as it highly depends on the saturation of the system, the
514 intensity of the precipitation event, the discharge of the River, and the type and frequency of

515 effluents. Therefore, guidelines for spring protection should account for the variability of the
516 vulnerability and resilience of the karst spring.

517 The investigation at the pilot scale is essential for upscaling purposes, where the integration of
518 field data into similar and/or regional scale models can allow for a better management of spring
519 water resources at a larger scale. In the future, the water deficit typical of these semi-arid
520 regions, will be exacerbated as forecasted by forward-flow simulations because of climate
521 change constraints. Therefore, the high-resolution monitoring yields a quantification of yearly
522 volumes of floodwaters that can be used for potential managed recharge (storage and recovery;
523 ASR;) during the high flow to decrease shortage during low flow periods. Additionally, the
524 identification of indicator parameters and spring response to different types of contamination
525 hazards can be used in the development of Early Warning Systems to be implemented for water
526 treatment and supply. The investigation of the pilot karst springs since 2014 allowed the
527 classification of the springs, and the identification of potential threats, while providing models to
528 act as support tools for decision-makers to alleviate the risks and ensure the sustainable
529 exploitation of spring water or the identification of alternative water resources. This study
530 highlights the importance of setting up monitoring networks and collecting high-resolution data
531 in poorly studied spring catchments to understand karst systems, calibrate and validate models,
532 and predict potential spring responses to variable input (recharge or contamination).

533 **6. Acknowledgments**

534 This work was funded by multiple grants and awards since 2014; USAID and National Academy
535 of Science (Peer Science; project award: 102881; Cycle 3), UNICEF (Award# 103924; Project#
536 25778), AUB; University Research Board (Award# 103951; Project# 25512) and KARMA
537 project (L-CNRS in the framework of the PRIMA program; Award# 103895; Project# 25713).

538 Moreover, Beirut and Mount Lebanon Water Establishment and The Litani Water Authority are
539 thanked to facilitate the installation of instruments and access to field sites. Prof. Jason J. Gurdak
540 is thanked for his contribution to the work. Michele Citton, Fouad Andari, and Emmanuel
541 Dubois are thanked for field data collection. Additionally, the committee members of the
542 municipalities of Sakiet El Misk- Bhersaf, Bikfaya-Mhaidseh, Ballouneh and Kfardebbiane
543 among others are acknowledged for their kind collaboration.

544 **7. Author contribution**

545 **Joanna Doummar**: Approach and methodology, funding, flow and transport simulations, and
546 writing; **Marwan Fahs**: Numerical simulations and review, **Michel Aoun**: Transport
547 simulations, field acquisition, writing; **Assaad Kassem**: Data processing and flow simulations,
548 writing; **Reda ElGhawi**: Field acquisition and data collection; **Jihad Othman and Mohamad**
549 **Alali**: Field acquisition and data processing.

550 **8. Competing interests**

551 No competing interests.

552 **9. References**

553 Alam, S., Borthakur, A., Ravi, S., Gebremichael, M., Mohanty, S. K. (2021), Managed aquifer
554 recharge implementation criteria to achieve water sustainability. *Science of the Total Environment*,
555 768, 144992, doi.org/10.1016/j.scitotenv.2021.144992.

556 Ahmed, N., Ye, M., Wang, Y., Greenhalgh, T., and K. Fowler (2021), Using $\delta^{18}\text{O}$ and $\delta^2\text{H}$ to
557 Detect Hydraulic Connection Between a Sinkhole Lake and a First-Magnitude Spring, *Groundwater*,
558 doi.org/10.1111/gwat.13105

559 Andreo, B., Goldscheider, N., Vadillo, I., Vías, J.M., Neukum, C., Sinreich, M., Jiménez, P.,
560 Brechenmacher, J., Carrasco, F., and H. Hötzl (2006), Karst groundwater protection: first application
561 of a Pan-European approach to vulnerability, hazard and risk mapping in the Sierra de Líbar
562 (Southern Spain). *Sci. Total Environ.* 357 (1–3), 54–73. doi.org/10.1016/j.scitotenv.2005.05.019.

563 Bailly-Comte, V., Martin, J. B., Jourde, H., Sreaton, E. J., Pistre, S. and A., Langston (2010), Water
564 exchange and pressure transfer between conduits and matrix and their influence on hydrodynamics of
565 two karst aquifers with sinking streams, *J. Hydrol.*, 386 (1–4), 55–66,
566 doi:10.1016/j.jhydrol.2010.03.005.

567 Bakalowicz, M. (2005). Karst groundwater: A challenge for new resources. *Hydrogeology*
568 *Journal*, 13(1), 148–160. doi.org/10.1007/s10040-004-0402-9

569 Barberá, J.A. and B. Andreo (2012), Functioning of a karst aquifer from S Spain under highly
570 variable climate conditions, deduced from hydrochemical records. *Environ Earth Sci* 65, 2337–2349.

571 Barbieri, M., Boschetti, T., Petitta, M., and M. Tallini (2005), Stable isotopes (2H , 18O
572 and $87\text{Sr}/86\text{Sr}$) and hydrochemistry monitoring for groundwater hydrodynamics analysis in a karst
573 aquifer (Gran Sasso, Central Italy), *Appl. Geochem.*, 20 2063-2081

574 Benischke, R. (2021), Review: Advances in the methodology and application of tracing in karst
575 aquifers. *Hydrogeol J* 29, 67–88. doi.org/10.1007/s10040-020-02278-9

576 Butscher, C., and P. Huggenberger (2008). Intrinsic vulnerability assessment in karst areas: A
577 numerical modeling approach. *Water Resources Research*, 44(3). doi: 10.1029/2007wr006277

578 Butscher, C., Auckenthaler, A., Scheidler, S., & Huggenberger, P. (2011). Validation of a numerical
579 indicator of microbial contamination for karst springs. *GroundWater*, 49(1), 66–76,
580 doi.org/10.1111/j.1745-6584.2010.00687.x

581 Chang, Y., Hartmann, A., Liu, L., Jiang, G., and J. Wu (2021), Identifying More Realistic Model
582 Structures by Electrical Conductivity Observations of the Karst Spring, *Water Resources*
583 *Research*, 57(4), doi.org/10.1029/2020WR028587

584 Chen, Z., Auler, A. S., Bakalowicz, M., Drew, D., Griger, F., Hartmann, J., Jiang, G., Moosdorf,
585 N., Richts, A., Stevanovic, Z., Veni, G., & Goldscheider, N. (2017). The World Karst Aquifer
586 Mapping project: concept, mapping procedure and map of Europe. *Hydrogeology*
587 *Journal*, 25(3), 771– 785. doi.org/10.1007/s10040-016-1519-3

588 Chen, Z., Hartmann, A., Wagener, T., and N. Goldscheider (2018). Dynamics of water fluxes and
589 storages in an Alpine karst catchment under current and potential future climate
590 conditions. *Hydrology and Earth System Sciences*, 22(7), 3807– 3823. doi.org/10.5194/hess-22-
591 3807-2018

592 Chen, Z., and N. Goldscheider (2014) Modeling spatially and temporally varied hydraulic behavior
593 of a folded karst system with dominant conduit drainage at catchment scale, Hochifen-Gottesacker
594 Alps, *J. Hydrol.*, 514, 41-52, 10.1016/j.jhydrol.2014.04.005

595 Chiffre, A., Degiorgi, F., Buleté, A. et al. (2016), Occurrence of pharmaceuticals in WWTP effluents
596 and their impact in a karstic rural catchment of Eastern France. *Environ Sci Pollut Res* 23, 25427–
597 25441, doi.org/10.1007/s11356-016-7751-5

598 Clemens, M., Khurelbaatar, G., Merz, R., Siebert C., van Afferden, M., and T. Rödiger (2020),
599 Groundwater protection under water scarcity; from regional risk assessment to local wastewater
600 treatment solutions in Jordan, *Sci. Total Environ.*, 706, 136066, 10.1016/j.scitotenv.2019.136066

601 Diffenbaugh, N. S., and F. Giorgi (2012), Climate change hotspots in the CMIP5 global climate
602 model ensemble, *Clim. Chang.*, 114, 813– 822, doi:10.1007/s10584-012-0570-x.

603 Doummar, J., and M. Aoun (2018b), Assessment of the origin and transport of four selected
604 emerging micropollutants sucralose, acesulfame-K, gemfibrozil, and iohexol in a karst spring during
605 a multi-event spring response, *Journal of Contaminant Hydrol.*, 215, 11-20
606 doi:10.1016/j.jconhyd.2018.06.003

607 Doummar, J. and M., Aoun (2018a), Occurrence of selected domestic and hospital emerging
608 micropollutants on a rural surface water basin linked to a groundwater karst catchment,
609 *Environmental Earth Sciences*, 77(9), 351, doi:10.1007/s12665-018-7536-x

610 Doummar, J., Hassan Kassem, A., and J. J. Gurdak (2018b), Impact of historic and future climate on
611 spring recharge and discharge based on an integrated numerical modelling approach: Application on
612 a snow-governed semi-arid karst catchment area, *J. Hydrol.*, 565, 636–649,
613 doi:10.1016/j.jhydrol.2018.08.062

614 Doummar, J., Margane, A., Geyer, T., and M. Sauter (2018a) Assessment of key transport
615 parameters in a karst system under different dynamic conditions based on tracer experiments: the
616 Jeita karst system, Lebanon. *Hydrogeol J.*, doi.org/10.1007/s10040-018-1754-x

617 Doummar, J., Geyer, T., Baierl, M., Nödler, K., Licha, T., and M. Sauter (2014), Carbamazepine
618 breakthrough as indicator for specific vulnerability of karst springs: Application on the Jeita spring,
619 Lebanon, *Appl. Geochem.*, 47, 150-156

620 Doummar, J., Sauter, M., and T. Geyer (2012a), Simulation of flow processes in a large scale karst
621 system with an integrated catchment model (Mike She) – Identification of relevant parameters
622 influencing spring discharge, *Journal of Hydrol.*, 426–427, 112–123,
623 doi:10.1016/j.jhydrol.2012.01.021, 2012. 465

624 Doummar, J., Noedler, K., Geyer, T. and M. Sauter (2012b), Assessment and Analysis of
625 Micropollutants (2010 - 2011). - Special Report No. 13 of Technical Cooperation Project "Protection

626 of Jeita Spring", prepared by Department of Applied Geology, University of Göttingen, Germany; 48
627 p.; Göttingen

628 Dubois E., Doummar J., Pistre S., and M. Larocque (2020) Calibration of a semi-distributed lumped
629 model of a karst system using time series data analysis: the example of the Qachqouch karst spring.
630 *Hydrol. Earth Syst. Sci.*, 24, 4275–4290, doi.org/10.5194/hess-24-4275-2020

631 Duran, L., and L. Gill (2021), Modeling spring flow of an Irish karst catchment using Modflow-USG
632 with CLN, *Journal of Hydrol.*, 597, 125971, doi.org/10.1016/j.jhydrol.2021.125971.

633 Einsiedl, F., Radke, M., and P. Maloszewski (2010), Occurrence and transport of pharmaceuticals in
634 a karst groundwater system affected by domestic wastewater treatment plants, *Journal of*
635 *Contaminant Hydrology*, 117, 26-36

636 ElGhawi, R., Pekhazis, K. and J. Doummar (2021), Multi-regression analysis between stable isotope
637 composition and hydrochemical parameters in karst springs to provide insights into groundwater
638 origin and subsurface processes: regional application to Lebanon. *Environ Earth Sci* 80, 230,
639 doi.org/10.1007/s12665-021-09519-4

640 El-Hakim, M. and M. Bakalowicz (2007), Significance and origin of very large regulating power of
641 some karst aquifers in the Middle East. Implication on karst aquifer classification, *Journal of*
642 *Hydrology*, 333(2–4), 329–339, doi:10.1016/j.jhydrol.2006.09.003, 2007.

643 Epting, J. M., Page, R., Auckenthaler, A., and P. Huguenberger (2018), Process-based monitoring
644 and modeling of Karst springs – linking intrinsic to specific vulnerability *Sci. Total Environ.*, 625,
645 403-415, 10.1016/j.scitotenv.2017.12.272

646 Fayad, A., Gascoin, S., Faour, G., López-Moreno, J. I., Drapeau, L., Le Page, M., and R. Escadafal
647 (2017). Snow hydrology in Mediterranean mountain regions: A review. *Journal of Hydrology*, 551,
648 374–396.

649 Fleury, S., 2009. Land use policy and practice in karst terrains. Springer.

650 Fleury, P., Ladouche, B., Conroux, Y. Jourde, H. and N. Dörfliger (2009), Modelling the hydrologic
651 functions of a karst aquifer under active water management – The Lez spring. *Journal of Hydrol.* 365
652 (3-4), 235-243. doi: 10.1016/j.jhydrol.2008.11.037.

653 Fleury, P., Maréchal, J.C., and B. Ladouche (2015). Karst flash-flood forecasting in the city of
654 Nîmes (southern France). *Eng. Geol.*, 164, 26-35

655 Ford, D., & Williams, P. (2007). Karst hydrogeology and geomorphology. West Sussex, England:
656 John Wiley & Sons Ltd., doi.org/10.1002/9781118684986

657 Frank, S., Goeppert, N. and N. Goldscheider (2018), Fluorescence-based multi-parameter approach
658 to characterize dynamics of organic carbon, faecal bacteria and particles at alpine karst springs,
659 *Sci. Total Environ.*, 615 1446-1459

660 Gao, Z., Liu, J. , Xu, X., Wang, Q., Wang, M., Feng, J., and T. Fu (2020), Temporal variations of
661 spring water in karst areas: a case study of jinan spring area, northern China, *Water*, 12 (4)

662 Gasser, G., Rona, M., Voloshenko, A., Shelkov, R., Tal, N., Pankratov, I., Elhanany, S., and Lev, O
663 (2010), Quantitative Evaluation of Tracers for Quantification of Wastewater Contamination of
664 Potable Water Sources, *Environmental Science & Technology* 44 (10), 3919-3925, doi:
665 10.1021/es100604c

666 Geyer, T., Birk, S., Licha, T., Liedl, R., and M. Sauter (2007), Multitracer test approach to
667 characterize reactive transport in karst aquifers. *Ground Water* 45(1): 36– 45.

668 Geyer, T., Birk, S., Licha, T., Liedl, R., and M. Sauter (2008), Quantification of temporal distribution
669 of recharge in karst systems from spring hydrographs, *J. Hydrol.*, 348, 452-463

670 Goderniaux, P., Brouyère, S., Wildemeersch, S., Therrien, R., and A. Dassargues (2015), Uncertainty
671 of climate change impact on groundwater reserves – application to a chalk aquifer. *J. Hydrol.*, 528,
672 108-121

673 Göppert, N., and N. Goldscheider (2007) Solute and colloid transport in karst conduits under low-
674 and high-flow conditions. *GroundWater*. doi.org/10.1111/j.1745-6584.2007.00373.x

675 Hartmann, A., Goldscheider, N., Wagener, T., Lange, J., and M. Weiler (2014b) Karst water
676 resources in a changing world: review of hydrological modeling approaches. *Rev. Geophys* 52, 218-
677 242. doi.org/10.1002/2013RG000443

678 Gutierrez, F., Parise, M., De Waele, J. and H. Jourde (2014) A review on natural and human-induced
679 geohazards and impacts in karst. *Earth Science Reviews*, 138, 61-88, doi:
680 10.1016/j.earscirev.2014.08.002.

681 Hartmann, A., Lange, J., Vivó, À., Mizyed, N., Smiatek, G., Vivó Aguado, À., Mizyed, N., Smiatek,
682 G., and H. Kunstmann (2012). A multi-model approach for improved simulations of future water
683 availability at a large Eastern Mediterranean karst spring. *J. Hydrol.* 468–469, 130–138.
684 doi:10.1016/j.jhydrol.2012.08.024

685 Hartmann, A., Mudarra, M., Andreo, B., Marín, A., Wagener, T., and J. Lange (2014a). Modeling
686 spatiotemporal impacts of hydroclimatic extremes on groundwater recharge at a Mediterranean karst
687 aquifer. *Water Resources Research*, 50(8), 6507-6521

688 Hartmann, A., Barberá, J. A., Lange, J., Andreo, B., and M. Weiler (2013a). Progress in the
689 hydrologic simulation of time variant recharge areas of karst systems—Exemplified at a karst spring
690 in Southern Spain. *Advances in Water Resources*, 54, 149-160.
691 doi.org/10.1016/j.advwatres.2013.01.010

692 Hartmann, A., Gleeson, T., Rosolem, R., Pianosi, F., Wada, Y., and T. Wagener (2015). A large-
693 scale simulation model to assess karstic groundwater recharge over Europe and the
694 Mediterranean. *Geoscientific Model Development*, 8(6), 1729– 1746, doi.org/10.5194/gmd-8-1729-
695 2015

696 Hartmann, A., Liu, Y., Olarinoye, T., Berthelin, R., & Marx, V. (2020). Integrating field work and
697 large-scale modeling to improve assessment of karst water resources. *Hydrogeology*
698 *Journal*. doi.org/10.1007/s10040-020-02258-z

699 Hartmann, A., Wagener, T., Rimmer, A., Lange, J., Brielmann, H., and M. Weiler (2013c). Testing
700 the realism of model structures to identify karst system processes using water quality and quantity
701 signatures. *Water Resources Research*, 49(6), 3345– 3358, doi.org/10.1002/wrcr.20229

702 Hartmann, A., Weiler, M., Wagener, T., Lange, J., Kralik, M., Humer, F., et al. (2013b). Process-
703 based karst modelling to relate hydrodynamic and hydrochemical characteristics to system
704 properties. *Hydrology and Earth System Sciences*, 17(8), 3505– 3521, doi.org/10.5194/hess-17-3305-
705 2013

706 Hartmann, A., Barberá, J.-A., and B. Andreo (2017), On the value of water quality data and
707 informative flow states in karst modeling *Hydrol. Earth Syst. Sci.*, 21, 5971-598

708 He, X., Wu, J. & Guo, W. (2019) Karst Spring Protection for the Sustainable and Healthy Living:
709 The Examples of Niangziguan Spring and Shuishentang Spring in Shanxi, China. *Expo*
710 *Health* 11, 153–165, doi.org/10.1007/s12403-018-00295-4

711 Heinz, B., Birk, S., Liedl, R., Geyer, T., Straub, K.L., Andresen, J., Bester, K., and A. Kappler
712 (2009), Water quality deterioration at a karst spring (Gallusquelle, Germany) due to combined sewer
713 overflow: evidence of bacterial and micro-pollutant contamination, *Environmental Geology*, 57 (4),
714 797-808

715 Hillebrand, O., Nödler, K., Sauter, M., and T. Licha (2015), Multitracer experiment to evaluate the
716 attenuation of selected organic micropollutants in a karst aquifer *Sci. Total Environ.*, 506–507, 338-
717 343, doi :10.1016/j.scitotenv.2014.10.102

718 Hillebrand, O., Nödler, K., Licha, T., Sauter, M., and T. Geyer (2012) Caffeine as an indicator for
719 the quantification of untreated wastewater in karst systems, *Water. Res.*, 46 (2), 395-402

720 Hou, D., Song, X., Zhang, and G. et al. (2013), An early warning and control system for urban,
721 drinking water quality protection: China's experience. *Environ Sci Pollut Res* 20, 4496–4508.
722 doi.org/10.1007/s11356-012-1406-y

723 Iglesias, A., Garrote, L., Flores, F., and M. Moneo (2007), Challenges to manage the risk of water
724 scarcity and climate change in the Mediterranean *Water Resour. Manage.*, 21, 775

725 Jódar, J., González-Ramón, A., Martos-Rosillo, S., Heredia, J., Herrera, C., Urrutia, J., Caballero,
726 Y., Zabaleta, A., Antigüedad, I., Custodio, E., and L.J. Lambán (2020), Snowmelt as a determinant
727 factor in the hydrogeological behaviour of high mountain karst aquifers: the Garcés karst system,
728 Central Pyrenees (Spain), *Sci. Total Environ.*, 748,141363, 10.1016/j.scitotenv.2020.141363

729 Jongman, B., Hochrainer-Stigler, S., Feyen, L., Aerts, J. C. J. H., Mechler, R., Wouter Botzen, W. J.,
730 Bouwer, L. M., Pflug, G., Rojas, R., and P. J. Ward (2014), Increasing stress on disaster-risk finance
731 due to large floods, *Nature Climate Change*, 4(4), 264-268.

732 Karnib, A. (2014) A methodological approach for quantitative assessment of the effective wastewater
733 management: Lebanon as a case study. *Environ Process* 1(4), 483–495. doi:10.1007/s40710-014-
734 0032-8

735 Käß W (1998) Tracing technique in geohydrology. Balkema, Rotterdam, The Netherlands, 589 pp

736 Kløve, B., Pertti Ala-Aho, P., Bertrand, G., Gurdak, J.J., Kupfersberger, H., Kværner, J., Muotka, T.,
737 Mykrä, H., Preda, E., Rossi, P., Bertacchi Uvo, C., Velasco, E., and M. Pulido-Velazquez (2014),

738 Climate change impacts on groundwater and dependent ecosystems, *Journal of Hydrology*, 518(B),
739 250-266, doi.org/10.1016/j.jhydrol.2013.06.037

740 Koeniger, P., Margane, A., Abi-Rizk, J., and T. Himmelsbach (2017). Stable isotope-based mean
741 catchment altitudes of springs in the Lebanon Mountains. *Hydrological Processes*, 31(21), 3708–
742 3718, doi.org/10.1002/hyp.11291

743 Koohbor, B., Fahs, M., Hoteit, H., Doummar, J., Younes, A. , and B. Belfort (2020) An advanced
744 discrete fracture model for variably saturated flow in fractured porous media, *Adv. Water*
745 *Resour.*, 140, 103602, doi:10.1016/j.advwatres.2020.103602

746 Korfali, S.I., and M. Jurdi (2009), Provision of safe domestic water for the promotion and protection
747 of public health: a case study of the city of Beirut, Lebanon. *Environ Geochem Hlth* 31: 283–295.

748 Kresic, N., and Z. Stevanović (2009), Groundwater Hydrology of Springs: Engineering, Theory,
749 Management and Sustainability, Butterworth-Heinemann, Oxford, U. K.

750 Liu, H., and G. Li (2020), Step-like rising and falling of a breakthrough curve observed at a karst
751 spring, *Journal of Contaminant Hydrology*, 235, doi.org/10.1016/j.jconhyd.2020.103726.

752 Luo, Q., Yang, Y., Qian, J., Wang, X., Chang, X., Ma, L., Li, F., and J. Wu (2020), Spring protection
753 and sustainable management of groundwater resources in a spring field, *J. Hydrol.*, 582, 124498,
754 doi.org/10.1016/j.jhydrol.2019.124498.

755 Mangin, A. (1975), Contribution à l'étude hydrodynamique des aquifères karstiques, Ph.D. thesis,
756 Université de Dijon, Dijon, France.

757 Marechal, J. -C., Vestier, A., Jourde, H. and N. Dorfliger (2013), L'hydrosysteme du Lez : une
758 gestion active pour un karst à enjeux. *Karstologia*, 62, 1-6.

759 Marín, A., I., Andreo, B., and M. Mudarra, (2015), Vulnerability mapping and protection zoning of
760 karst springs. Validation by multitracer tests, *Science of The Total Environment*, 435-446,
761 doi.org/10.1016/j.scitotenv.2015.05.029.

762 Marín, A.I., Martín Rodríguez, J.F., Barberá, J.A. et al. (2021), Groundwater vulnerability to
763 pollution in karst aquifers, considering key challenges and considerations: application to the Ubrique
764 springs in southern Spain. *Hydrogeol J.* 29, 379–396, doi.org/10.1007/s10040-020-02279-8

765 Massoud, M.A., Tareen, J., Tarhini, A. et al. (2010), Effectiveness of wastewater management in
766 rural areas of developing countries: a case of Al-Chouf Caza in Lebanon. *Environ Monit*
767 *Assess* 161, 61–69, doi.org/10.1007/s10661-008-0727-2

768 Mazzilli, N. Guinot, V. Jourde, H., Lecoq, N., Labat, D.,
769 Arfib, B., Baudement, C., Danquigny, C., Dal Soglio, L., and D. Bertin (2017), KarstMod: A
770 modelling platform for rainfall - discharge analysis and modelling dedicated to karst systems,
771 *Environ. Model. Softw.*, 1–7, doi10.1016/j.envsoft.2017.03.015

772 Moeck, C., Grech-Cumbo, N., Podgorski, J., Bretzler, A., Gurdak, J.J., Berg, M., Schirmer, M.,
773 (2020), A global-scale dataset of direct natural groundwater recharge rates: A review of variables,
774 processes and relationships, *Science of the Total Environment* (717),
775 doi.org/10.1016/j.scitotenv.2020.137042

776 Mudarra, M. Hartmann, A. Andreo, B. (2019), Combining Experimental Methods and Modeling to
777 Quantify the Complex Recharge Behavior of Karst Aquifers. *Water Resources Research*, 55(2),
778 1384-1404.

779 Mudarra, M., Andreo, B., and J. Mudry (2010), Hydrochemical heterogeneity in the discharge zone
780 of a karstic aquifer. In: Andreo B, Carrasco F, Durán JJ, LaMoreaux JW (eds) *Advances in research*
781 *in Karst media*. Springer, Berlin, 163–168

782 Mudarra, M., B. Andreo and J. Mudry, (2012), Monitoring groundwater in the discharge area of a
783 complex karst aquifer to assess the role of the saturated and unsaturated zones, *Environmental Earth*
784 *Sciences*, 65(8), 2321 doi: 10.1007/s12665-011-1032-x

785 Nerantzaki, S. D., and N.P. Nikolaidis (2020), The response of three Mediterranean karst springs to
786 drought and the impact of climate change, *J. Hydrol.*, 591 (2020),
787 125296, doi:10.1016/j.jhydrol.2020.125296

788 North, L.A., van Beynen, P.E., Parise, M., 2009. Interregional comparison of karst disturbance: west-
789 central Florida and southeast Italy. *J. Environ. Manag.* 9 (5), 1770–1781.

790 Olarinoye, T., Gleeson, T., Marx, V. et al. (2020), Global karst springs hydrograph dataset for
791 research and management of the world’s fastest-flowing groundwater. *Sci Data* 7, 59
792 doi.org/10.1038/s41597-019-0346-5

793

794 Parise, M., Closson, D., Gutiérrez, F. and Z. Stevanovic (2015), Anticipating and managing
795 engineering problems in the complex karst environment. *Environ Earth Sci* 74, 7823-7835.
796 doi.org/10.1007/s12665-015-4647-5

797 Parise, M., Gabrovsek, F., Kaufmann, G., and N. Ravbar (2018) Recent advances in karst research:
798 from theory to fieldwork and applications. In: Parise M, Gabrovsek F, Kaufmann G, Ravbar N (eds.)
799 Advances in Karst research: theory, fieldwork and applications. Geological society, London, Special
800 Publications, 466, 1-24, doi.org/10.1144/SP466.26

801 Perrin, J., Jeannin, PY., and F. Zwahlen (2003). Epikarst storage in a karst aquifer: a conceptual
802 model based on isotopic data, Milandre test site, Switzerland. *J Hydrol* 279,106–124

803. Petitta, M., Barberio, D. M., Barbieri, M., Billi, A., Doglioni, C., Passaretti, S., and S. Franchini
804 (2020), Groundwater monitoring in regional discharge areas selected as “Hydrosensitive” to seismic
805 activity in Central Italy. in *Advances in Natural Hazards and Hydrological Risks: Meeting the*
806 *Challenge 21–25* (Springer, New York, 2020).

807 Pronk, M., Goldscheider, N. and J. Zopfi (2006), Dynamics and interaction of organic carbon,
808 turbidity and bacteria in a karst aquifer system, *Hydrogeol J.* 14, 473–484. doi.org/10.1007/s10040-
809 005-0454-5

810 Rusjan, S., Sapač, K., Petrič, M., Lojen, S., and N. Bezak (2019) Identifying the hydrological
811 behavior of a complex karst system using stable isotopes. *J Hydrol* 577, 123956

812 Sauter, M. (1992), Quantification and forecasting of regional groundwater flow and transport in a
813 karst aquifer (Gallusquelle, Malm, SW Germany), *Tubinger Geowissenschaftliche Arbeiten, Part*
814 *C* (13) (1992), p. 151

815 Scanlon, B.R., R.E. Mace, M.E. Barrett, B. Smith (2003), Can we simulate regional groundwater
816 flow in a karst system using equivalent porous media models? Case study, Barton Springs Edwards
817 aquifer USA, *J. Hydrol.*, 276, 137-158, 10.1016/S0022-1694(03)00064-7

818 Schmidt, S., Geyer, T., Marei, A., Guttman, J., and M. Sauter (2013), Quantification of long-term
819 wastewater impacts on karst groundwater resources in a semi-arid environment by chloride mass
820 balance methods, *J. Hydrol*, 502, 177-190, 10.1016/j.jhydrol.2013.08.009

821 Schnegg, PA (2002), An inexpensive field fluorometer for hydrogeological tracer tests with three
822 tracers and turbidity measurement. In: Bocanegra E, Martinez D, Massone H (ed) *Proc. of the*
823 *XXX/IAH Congress Groundwater and Human Development. Mar Del Plata, Argentina, October*
824 *2002*, 1484–1488

825 Siirila-Woodburn, E. R., D. Fernandez Garcia, and X. Sanchez-Vila (2015), Improving the accuracy
826 of risk prediction from particle-based breakthrough curves reconstructed with kernel density
827 estimators. *Water Resour. Res.*, 51, 4574–4591

828 Sivellev, V., Jourde, H., Bittner, D., Mazzilli, N., and Y. Trambly (2021), Assessment of the relative
829 impacts of climate changes and anthropogenic forcing on spring discharge of a Mediterranean karst
830 system, *Journal of Hydrol.*, 598, 126396, doi.org/10.1016/j.jhydrol.2021.126396.

831 Sivellev, V., Renard, P., Labat D., (2020), Coupling SKS and SWMM to Solve the Inverse Problem
832 Based on Artificial Tracer Tests in Karstic Aquifers, *Water*, 12, 1139, 10.3390/w12041139

833 Stange, C. and A. Tiehm (2020), Occurrence of antibiotic resistance genes and microbial source
834 tracking markers in the water of a karst spring in Germany, *Sci. Total Environ.*, 742,
835 140529, doi:10.1016/j.scitotenv.2020.140529

836 Stedmon C A., Seredyńska-Sobecka B., Boe-Hansen R, Le Tallec N., Christopher K.Waul C.K.,
837 Arvinb E. (2011), A potential approach for monitoring drinking water quality from groundwater
838 systems using organic matter fluorescence as an early warning for contamination events. *Water*
839 *Resources*, 45. 6030-6038, doi.org/10.1016/j.watres.2011.08.066

840 Stevanović, Z. (2015), *Karst Aquifers – Characterization and Engineering*. Springer, Cham,
841 Switzerland

842 Stevanović, Z. (2019a), Karst waters in potable water supply: a global scale overview, *Environ.*
843 *Earth Sci.*, 78, 1-12, 10.1007/s12665-019-8670-9

844 Stevanović Z. (2019b) Karst Aquifers in the Arid World of Africa and the Middle East:
845 Sustainability or Humanity?. In: Younos T., Schreiber M., Kosič Ficco K. (eds) *Karst Water*
846 *Environment*. The Handbook of Environmental Chemistry, vol 68. Springer, Cham.
847 https://doi.org/10.1007/978-3-319-77368-1_1

848 Stevanović, Z., and A. M. Stevanović (2021), Monitoring as the Key Factor for Sustainable Use and
849 Protection of Groundwater in Karst Environments—An Overview, *Sustainability*, 13(10), 5468,
850 doi:10.3390/su13105468.

851 Toride N., Leij F. J., van Genuchten (1999), The CXTFit code for estimating transport parameters
852 from laboratory or field tracer experiments. Version 2.1. Res. Rep. 137. US- Riverside CA

853 Torresan, F., Fabbri, P., Piccinini, L., Dalla Libera, N., Pola, M., and D. Zampieri, (2020), Defining
854 the hydrogeological behavior of karst springs through an integrated analysis: a case study in the
855 Berici Mountains area (Vicenza, NE Italy), *Hydrogeol. J.* 1-19

856 Van Beynen, P.E., Townsend, K.M., 2005. A disturbance index for karst environments. *Environ.*
857 *Manag.* 36 (1), 101–116.

858 Van Loon, A. F., Kumar, R., and V. Mishra (2017), Testing the use of standardised indices and
859 GRACE satellite data to estimate the European 2015 groundwater drought in near-real time.
860 *Hydrology Earth System Sciences*, 21(4), 1947-1971.

861 Van Stempvoort, D.R., Roy, J.W., Grabuski, J., Brown, S.J., Bickerton, G. and E. Sverko (2013)
862 An artificial sweetener and pharmaceutical compounds as co-tracers of urban wastewater in
863 groundwater, *Sci. Total Environ.*, 461-462, 348-359

864 Wang, F., Chen, H., Lian, J., Fu, Z., and Y. Nie (2020), Seasonal recharge of spring and stream
865 waters in a karst catchment revealed by isotopic and hydrochemical analyses, *J. Hydrol.*, 591,
866 125595, 10.1016/j.jhydrol.2020.125595

867 Warner, W., Licha, T., and K. Nödler (2019), Qualitative and quantitative use of micropollutants as
868 source and process indicators. A review, *Science of The Total Environment*, 686, 75-89,
869 doi.org/10.1016/j.scitotenv.2019.05.385

870 Worthington S.R.H. (1999) A comprehensive strategy for understanding flow in carbonate aquifers.
871 In: Palmer A.N., Palmer M.V. & Sasowsky I.D. (Eds.), Karst modeling. Karst Water Institute, special
872 publication 5, p. 30-37.

873 Zirlewagen, J, Licha, T., Schiperski F., Noedler, K., and T. Schyett (2016), Use of two artificial
874 sweeteners, cyclamate and acesulfame, to identify and quantify wastewater contributions in a karst
875 spring, *Sci. Total Environ.*, 547. 356-365

876